Sustainable Energy & Fuels

ROYAL SOCIETY OF CHEMISTRY

PAPER

Cite this: *Sustainable Energy Fuels*, 2021, **5**, 3467

Optimizing two green-like biomass pretreatments for maximum bioethanol production using banana pseudostem by effectively enhancing cellulose depolymerization and accessibility†

Fei Liu,[ab] Jingyang Li,[ac] Hua Yu,[ab] Yuqi Li,[b] Yanting Wang,[ab] Hairong Gao,[ab] Hao Peng,[ab] Zhen Hu,[ab] Hailang Wang,[ab] Guifen Zhang,[ab] Yuanyuan Tu[ab] and Liangcai Peng*[ab]

The banana is an important fruit crop that generates enormous quantities of lignocellulose-rich pseudostem residues that can be converted into biofuels and biochemicals. By performing response surface methodological modeling, optimized green liquor (GL) and liquid hot water (LHW) pretreatments of representative banana samples were studied. Using banana (BP-1) pseudostem residues rich in directly fermentable soluble sugars (27% hexoses and 2.7% pentoses *via* dry matter) and easily digestible xyloglucans, we measured nearly complete enzymatic saccharification with a hexose yield of 99% (% cellulose) from the most optimal GL pretreatment under relatively mild conditions. Notably, both optimal LHW (20 min, 110 °C) and GL (26.74% TTA, 105 °C, 26 min) pretreatments led to the highest bioethanol yields achieved thus far, at 27% and 31% (% dry matter), respectively, subjective to yeast fermentation with all hexose sources obtained in the BP-1 sample. Furthermore, we determined that optimal LHW and GL pretreatments extracted lignin by 25% and 40%, and reduced the cellulose crystalline index by 35% and 44% and polymerization degree by 34% and 36%, respectively, with distinctively altered lignin and hemicellulose features. Cellulose accessibility was increased 2–3 fold for remarkably enhanced enzymatic saccharification of biomass. Hence, we propose a mechanism model to elucidate why banana lignocellulose underwent complete biomass enzymatic saccharification under mild green-like pretreatments, providing an applicable strategy that can be used to produce large quantities of bioethanol from banana lignocellulose residues and beyond.

Received 21st April 2021
Accepted 31st May 2021

DOI: 10.1039/d1se00613d

rsc.li/sustainable-energy

1. Introduction

Plants conduct photosynthesis to convert solar energy into chemical energy that is storable in lignocellulose, providing the most abundant biomass on Earth.[1,2] Because of the ongoing efforts to reduce globe warming and overconsumption of fossil fuels, lignocellulose is increasingly being considered for conversion to create renewable and sustainable bioenergy.[3] Importantly, lignocellulose ethanol has been evaluated as a promising second generation of bioenergy that will be able to partially replace fossil fuels.[4,5] However, due to lignocellulose recalcitrance, bioethanol production requires costly lignocellulose enzymatic saccharification.[6–8]

In principle, lignocellulose recalcitrance is defined by plant cell wall composition, cell wall polymer characteristics, and cell wall-network construction.[9] In particular, cellulose crystallinity and polymerization are two major factors that negatively affect enzymatic saccharification of biomass, whereas hemicellulose can reduce cellulose crystallinity.[10–14] Despite lignin being a barrier against cellulase accession, three lignin monomers (S, G, H) play distinct roles in the enzymatic hydrolyses of lignocellulose.[15]

To reduce lignocellulose recalcitrance, physical and chemical pretreatments have been extensively performed as initial steps for sequential enzymatic hydrolysis and final bioethanol production.[16] However, most pretreatments have been performed under extreme conditions, and the production of secondary wastes could not be avoided.[17–19] Alternatively, green-like pretreatments have been implemented using industrial chemical wastes or non-chemical liquid hot water.[20] For

[a]*Biomass & Bioenergy Research Centre, College of Plant Science & Technology, Huazhong Agricultural University, Wuhan 430070, China. E-mail: lpeng@mail.hzau.edu.cn; Web: http://bbrc.hzau.edu.cn; Fax: +86-27-87280016; Tel: +86-27-87281765*

[b]*Laboratory of Biomass Engineering & Nanomaterial Application in Automobiles, College of Food Science & Chemical Engineering, Hubei University of Arts and Science, Xiangyang 441053, China*

[c]*Haikou Experimental Station, Chinese Academy of Tropical Agricultural Sciences, Haikou 570102, China*

† Electronic supplementary information (ESI) available. See DOI: 10.1039/d1se00613d

instance, green liquor (GL) has been broadly applied to pretreat various lignocellulose residues using a smelt solution (a mixture of sodium carbonate and sodium sulfide) obtained from a recovery boiler in a kraft pulp mill.[21–23] More recently, green liquor pretreatment has been applied to selectively remove major lignin components for hemicellulose and cellulose collection, with the advantage of much less generation of toxic or corrosive byproducts. However, the optimal conditions for green-like pretreatments for banana biomass processes have not yet been determined.[24]

Bananas are an important fruit crop all over the world, providing sufficient carbohydrates with high nutrition, and banana plants produce enormous pseudostem residues rich in lignocellulose.[25–29] Although there have been recent attempts to increase banana pseudostem utilization,[30] little has been reported regarding its optimal conversion for biofuels, in particular, for achieving high yields of bioethanol from banana residues. Using two banana pseudostem samples with high cellulose and lignin levels, we established two optimized green-like pretreatments by performing response surface methodology (RSM) analysis.[31,32] Hence, we determined in this study why the banana pseudostems underwent complete enzymatic digestion with maximum bioethanol production after undergoing two optimal green-like pretreatments.

2. Materials and methods

2.1. Banana pseudostem collection

Banana plants were grown in the Banana Experimental Field of the Haikou Experimental Station, Chinese Academy of Tropical Agricultural Sciences, Danzhou, Hainan. After banana fruits were harvested, the remaining pseudostem residues were chopped and dried at 60 °C until constant weight was achieved. The dried pseudostem samples were ground into powders, passed through a 40-mesh screen, and stored in a dry container pending use.

2.2. Wall polymer extraction and assay

Plant cell wall fractionation was performed to extract major wall polymers, as previously described.[33] After successive extractions of soluble sugars, lipids, and starch by phosphate buffer (pH 7.0), chloroform–methanol (1 : 1, v/v), and dimethyl sulfoxide (DMSO)–water (9 : 1, v/v), the remaining crude cell wall pellets were incubated with 0.5% ammonium oxalate monohydrate (w/v) for 1 h in a boiling water bath to extract the pectin fraction. The remaining residues were incubated with 4 M KOH (containing 1.0 mg mL^{-1} sodium borohydride) at 25 °C for 1 h, and the supernatants were collected as KOH-extractable hemicellulose fractions after centrifugation at 4000*g*. The remaining non-KOH extractable residues were dissolved with H_2SO_4 (67%, v/v) at 25 °C for 1 h, and the hexose of the supernatants was detected as the cellulose fraction. Total hexoses and pentoses of the KOH-extractable hemicelluloses and pentoses of the non-KOH extractable fraction were summed as the hemicellulose content. Total hexoses, pentoses, and uronic acids were summed as the pectin level. A UV-Vis spectrometer (V-1100D, Shanghai MAPADA Instruments Co., Ltd, Shanghai, China) was used to detect hexoses, pentoses, and uronic acids as previously described.[13] A two-step acid hydrolysis method was applied for detection of lignin content according to the Laboratory Analytical Procedure of the National Renewable Energy Laboratory (NREL), as previously described.[34] All experiments were performed in independent triplicate.

2.3. Determination of hemicellulose monosaccharides and lignin monomers

Monosaccharides of hemicelluloses were determined by GC-MS (Shimadzu GCMS-QP2010 Plus) using a Restek Rxi-5ms, 30 m × 0.25 mm ID × 0.25 μm df column with a mass spectrometer operated in electron ionization (EI) mode with ionization energy of 70 eV.[35,36] Calibration curves of all analytes routinely yielded correlation coefficients of 0.999 or better. Monomers of lignin were detected by HPLC (1525, Waters Corp., MA, USA) as previously described.[37]

2.4. Fourier transform infrared spectroscopic profiling

A PerkinElmer spectrophotometer (NEXUS 470, Thermo Fisher Scientific, Waltham, MA, USA) was applied to qualitatively monitor the biomass samples, and the FTIR spectra were recorded in absorption mode over 32 scans at a resolution of 4 cm^{-1} in the range of 4000 to 400 cm^{-1} regions as previously described.[11]

2.5. Measurement of cellulose features (CrI, DP) and accessibility

The cellulose crystalline index (CrI) was measured with a Rigaku-D/MAX instrument (Ultima III, Japan) using the equation: $CrI = 100 \times (I_{200} - I_{am})/I_{200}$. I_{200} denotes the intensity of the 200 peak (I_{200}, $\theta = 22.5°$), which represents crystalline cellulose, whereas I_{am} (I_{am}, $\theta = 18.5°$) denotes the intensity at the minimum between the 200 and 110 peaks, corresponding to amorphous cellulose. The degree of polymerization (DP) of cellulose samples was determined using the viscosity method, which is expressed by the equation: $DP^{0.905} = 0.75[\eta]$, as previously described.[38] All experiments were performed in independent triplicate at 25 ± 0.5 °C. Cellulose accessibility was estimated by performing Congo red (CR) staining, as previously described[39] with minor modification.[38] The samples (0.1 g) were incubated with dye solution in a series of increasing concentrations (0.5, 1.0, 1.5, 2.0, 4.0, 6.0 mg mL^{-1}) in 0.3 M phosphate buffer (pH 6) with 1.4 mM NaCl at 60 °C for 24 h. After centrifugation at 8000*g*, the absorbance of the supernatant was measured at 498 nm, and the maximum amount of adsorbed dye was calculated by subtraction of free dye in the supernatant from the initially added dye.

2.6. Soluble sugar extraction and assay

The biomass sample (0.3 g) was incubated with 6 mL potassium phosphate buffer (pH 4.8) in a boiling water bath for 1 h, with shaking every 10 min. After centrifugation at 3000*g* for 5 min, the supernatant was collected for experiments of enzymatic

hydrolysis and yeast fermentation. Hexoses and pentoses of soluble sugars were assayed using a colorimetric method as previously described.[40]

2.7. Biomass pretreatments

2.7.1. Green liquor (GL) pretreatment. GL solution was prepared by mixing Na_2S and Na_2CO_3 with a sulfidity (percent ratio of Na_2S to the sum of Na_2S and Na_2CO_3 on the basis of Na_2O) of 30%, as previously described.[41] The total titratable alkali (TTA, sum of Na_2S and Na_2CO_3, as Na_2O) charges on the oven-dried biomass ranged from 0% to 50% (w/w). The samples (0.3 g) were incubated with 2.4 mL GL solution in PTFE jars loaded with stainless steel bombs, and then treated in a lab-scale electrically heated oil bath while being stirred at 20 rpm. The temperature was raised at the rate of 3 °C min^{-1} to the target temperature (68–152 °C) and maintained for the scheduled time (8–42 min). After being cooled to room temperature, the pretreated residues were washed with distilled water until pH 7.0 was attained for the following enzymatic hydrolysis.

2.7.2. Experimental design and statistical analysis for optimizing GL pretreatment. To optimize GL pretreatment, the central composite rotatable design (CCRD) of response surface methodology (RSM) was performed with TTA (X_1), residence time (X_2), and pretreatment temperature (X_3) as independent factors/variables, and enzymatic hydrolysis as the response variable (Y). The experimental design was carried out with twenty trials, including six trials of the central point. All experiments were completed in independent triplicate to maintain the accuracy and reproducibility of the model, and their mean values were used as the response values. Linear regression analysis of the experimental data was performed to fit the second-order polynomial equation for the response variables, as given below:

$$Y = \beta_0 + \beta_1X_1 + \beta_2X_2 + \beta_3X_3 + \beta_4X_1X_2 + \beta_5X_1X_3 + \beta_6X_2X_3 + \beta_7{X_1}^2 + \beta_8{X_2}^2 + \beta_9{X_3}^2 \quad (1)$$

where Y denotes the dependent (response) variable; X_1, X_2, and X_3 denote the coded values for TTA (%), time (min), and temperature (°C), respectively; β_0 denotes a constant; β_1, β_2, and β_3 denote linear coefficients; β_4, β_5, and β_6 denote interaction coefficients; and β_7, β_8, and β_9 denote the quadratic coefficients of X_1, X_2, and X_3, respectively. The statistical significance of the model was determined by evaluating the P-value (<0.05) obtained from the analysis of variance (ANOVA). The quality of the model developed was evaluated by the coefficient of determination (R^2). The fitted polynomial equations obtained from the regression analysis were then expressed in the form of three-dimensional surface plots to illustrate the relationship between the responses and any two variables to be optimized. Furthermore, the numerical optimization method was used to calculate the optimal conditions with the assistance of Microsoft Excel. If there are multiple solutions to the equation and there are several optimal conditions, the one with the least sum of arithmetic squares was selected as the optimal. Confirmatory experiments under optimized conditions for GL pretreatment were carried out in triplicate for hexose yields after GL pretreatment of banana pseudostems to confirm the authenticity of the model generated.

2.7.3. Liquid hot water (LHW) pretreatment. The samples (0.3 g) were added to 2.4 mL distilled water in PTFE jars loaded with stainless steel bombs, and then treated at a solid/liquid ratio of 1 : 8 (w/v) in a lab-scale electrically heated oil bath containing 6 stainless steel bombs stirred at 20 rpm, as previously described.[11] The temperature was raised at the rate of 3 °C min^{-1} to the target temperature (75–145 °C), which was then maintained for the scheduled time (10–40 min). After being cooled to room temperature, the pretreated residues were washed with distilled water until pH 7.0 was attained for the following enzymatic hydrolysis.

2.7.4. Experimental design and statistical analysis for optimizing LHW pretreatment. To optimize the LHW pretreatment, the CCRD of RSM was performed with residence time (X_1) and pretreatment temperature (X_2) as independent factors/variables, and enzymatic hydrolysis as the response variable (Y). The experimental design was carried out with thirteen trials, including five trials of the central point. All experiments were performed in independent triplicate to maintain the accuracy and reproducibility of the model, and their mean values were considered as the response values. Linear regression analysis of the experimental data was performed to fit the second-order polynomial equation for the response variables as given below:

$$Y = \beta_0 + \beta_1X_1 + \beta_2X_2 + \beta_3X_1X_2 + \beta_4{X_1}^2 + \beta_5{X_2}^2 \quad (2)$$

where Y denotes the dependent (response) variable; X_1 and X_2 denote the coded values for time (min) and temperature (°C), respectively; β_0 denotes a constant; β_1 and β_2 denote linear coefficients; β_3 denotes an interaction coefficient; and β_4 and β_5 denote the quadratic coefficients of X_1 and X_2, respectively. The statistical significance of the model was determined by evaluating the P-value (<0.05) obtained from the analysis of variance (ANOVA). The quality of the model developed was evaluated by the coefficient of determination (R^2). The fitted polynomial equations obtained from the regression analysis were then expressed in the form of three-dimensional surface plots to illustrate the relationship between the responses and any two variables to be optimized, maintaining the other variable at the center point (constant). Furthermore, the numerical optimization method was used with Microsoft Excel to calculate the optimal conditions, as previously described. Confirmatory experiments under optimized conditions for LHW pretreatment were carried out in independent triplicate for hexose yields after LHW pretreatment of banana pseudostems to confirm the authenticity of the model generated.

2.8. Enzymatic hydrolysis

Enzymatic hydrolysis was conducted as previously described.[42] The pretreated materials were washed 3–5 times with distilled water (until pH 7 was attained) and once with 0.2 M phosphate buffer (pH 4.8). The biomass residues were then incubated with 6 mL (2 g L^{-1}) mixed-cellulase enzymes (Imperial Jade Biotechnology Co., Ltd, Ningxia, China) with final concentrations of cellulases at 21.20 FPU g^{-1} biomass and xylanase at

13.44 U g^{-1} biomass in a solution containing 1% Tween-80 at 5% solid loading, with 150 rpm agitation for 48 h at 50 °C. The samples were centrifuged at 3000*g* for 5 min, and the supernatants were collected for hexose and pentose assay. All experiments were carried out in independent triplicate.

2.9 Yeast fermentation for bioethanol production

Yeast fermentation and ethanol measurement were conducted as previously described.[10] *Saccharomyces cerevisiae* (purchased from Angel Yeast Co., Ltd, Yichang, China) was incubated with the enzymatic hydrolysis liquid to achieve a final concentration of 0.5 g L^{-1} in all fermentation tubes, and the fermentation was conducted at 37 °C for 48 h. Ethanol was measured using the $K_2Cr_2O_7$ method. The experiments were performed in independent triplicate. The sugar–ethanol conversion rates were calculated using the following equation:

$$\text{S} - \text{E}\ (\%) = \frac{E}{A \times H} \times 100 \quad (3)$$

where S–E (%) denotes the sugar–ethanol conversion rate; E denotes the total ethanol weight (g) at the end of fermentation; A denotes the theoretical conversion rate at 51.11% (92/180) in the case when glucose is completely converted to ethanol according to the Embden–Meyerhof–Parnas pathway in *S. cerevisiae*; and H denotes the total hexose weight (g) at the beginning of fermentation. All experiments were performed in independent triplicate.

2.10 Statistical analysis

Analyses of variance (ANOVA) and determinations of regression coefficients and Spearman's rank correlation coefficient were carried out using Superior Performance Software System (SPSS version 16.0, Inc., Chicago, IL, USA). Pair-wise comparisons were conducted between two measurements using Student's *t*-test. The line graph, histogram, and regression analysis for the best fit curve were generated using Origin 8.5 software (Microcal Software, Northampton, MA, USA). The RSM parameters were optimized using Design-Expert (software version v8.0.6, Stat-Ease, Inc., Minneapolis, MN, USA). The average values were calculated from the original triplicate measurements for these analyses.

3. Results and discussion

3.1. Optimizing GL and LHW pretreatments with two representative banana pseudostem samples

With the diversity of banana varieties, we selected two pseudostem samples (BP-1 and BP-2) containing high cellulose and lignin levels, respectively, for the experiments conducted in this work. By means of the classic RSM-based modeling approach, we optimized the influential factors of two green-like (GL, LHW) pretreatments with two representative pseudostem samples for enhancing biomass saccharification, measured by taking into account the hexose yields (% dry matter) released from the enzymatic hydrolyses of pretreated lignocellulose residues, as previously described.[41]

As a result, the influential factors included total titratable alkali (TTA, sum of Na_2S and Na_2CO_3, as Na_2O) and incubation temperature/time for the GL pretreatment, whereas the incubation time and temperature were optimized for the LHW (Fig. 1). Based on ANOVA, significant regression models with high coefficient of determination (R^2) values from 0.93 to 0.98 (Tables S1 and S2†) were created for both green-like treatments. In terms of hexose yields, the predicted and measured values exhibited a difference of less than 1%, indicating extremely accurate predictions of hexose yields for the two pseudostem samples under each green-like pretreatment. Furthermore, the

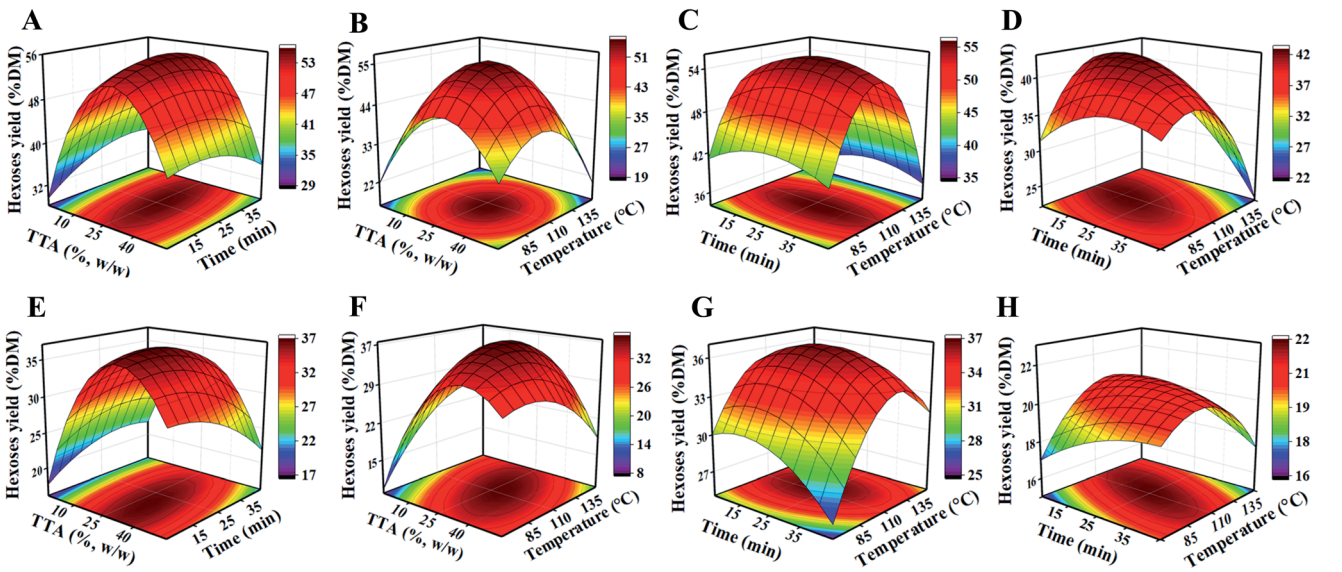

Fig. 1 Response surface diagrams of the effects of green liquor (GL) and liquid hot water (LHW) pretreatments on the hexose yields released after enzymatic saccharification of the pretreated biomass residues from samples of BP-1 and BP-2. (A)–(C) GL pretreatment of BP-1; (D) LHW pretreatment of BP-1; (E)–(G) GL pretreatment of BP-2; and (H) LHW pretreatment of BP-2; % dry matter (DM).

Table 1 Optimal conditions for green liquor and liquid hot water pretreatments with two banana pseudostem samples[a]

Samples	Pretreatments	Incubation conditions		
		Time (min)	Temperature (°C)	TTA (%, w/w)
BP-1	GL	26	105	26.71
	LHW	20	110	—
BP-2	GL	20	110	29.20
	LHW	24	112	—

[a] GL: green liquor pretreatment. LHW: liquid hot water pretreatment.

three-dimensional (3D) surface plots revealed that the individual factors and their interactive impacts on the responses (hexose yields) resulted in the other factors maintaining constant positions at their center points (Fig. 1).

The sugar yields released from the BP-1 sample were higher than those of BP-2 under the two green-like pretreatments performed in this study. However, relatively higher sugar yields were obtained with the GL pretreatment as compared to the LHW pretreatment, suggesting that the GL pretreatment should be more effective for banana biomass processing. Hence, this study determined the optimal conditions for GL and LHW pretreatments (Table 1), which could lead to greatly increased biomass enzymatic saccharification in the two banana pseudostem samples. We also confirmed that RSM-based modeling is a powerful approach for optimization of biomass pretreatments in banana and other bioenergy crops.

3.2. Maximized bioethanol production by subjecting banana pseudostems to optimal green-like pretreatments

Given the optimal green-like pretreatments that were performed for enhancing biomass enzymatic saccharification as

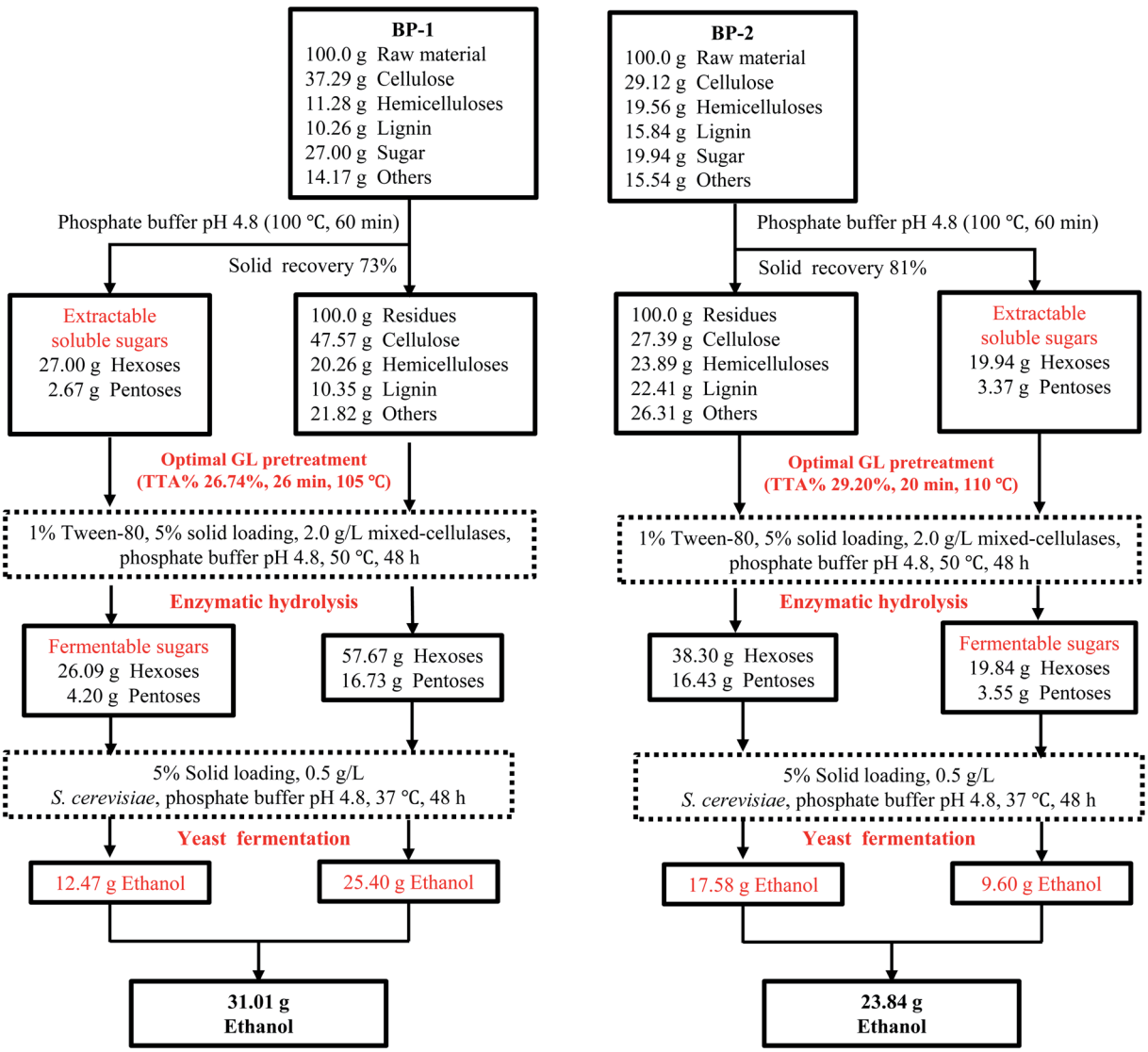

Fig. 2 Mass balance analysis of biomass processing for bioethanol production after performing optimal GL pretreatments of BP-1 and BP-2 samples.

described above, we conducted full biomass balance analyses of the two banana pseudostem samples used for bioethanol production (Fig. 2 and 3). Under the optimal GL pretreatment, the BP-1 sample released 57.67 g hexoses from the enzymatic hydrolysis of 100 g raw pseudostem material, whereas the hexose yield of the BP-2 sample was only 38.30 g, even though its optimal pretreatment required relatively stronger conditions (29.20% TTA, 110 °C) than those for the BP-1 sample (26.74% TTA, 105 °C). Despite the large variation in the hexose yields between BP-1 and BP-2, there were similar pentose yields (16.73 g and 16.43 g) for the two pseudostem samples. Notably, we determined that the raw material of the BP-1 sample contained 27% (% dry matter) soluble hexoses, which were directly fermentable for bioethanol production. In addition, the BP-2 sample contained 20% (% dry matter) fermentable hexoses, indicating that the banana pseudostems contain larger quantities of unique fermentable hexoses as compared to other crop straws, except sugarcane and sweet sorghum, as previously examined.[11,12,20,27,30,43–51]

Using our well-established approach,[10–12] a classic yeast fermentation was performed with all hexoses obtained from the enzymatic hydrolyses of extractable soluble sugars and pretreated lignocellulose residues from the two banana pseudostem samples, and their ethanol yields were finally calibrated according to the recovery rates of pretreated biomass performed in this study (Fig. 2), which was summarized using the mass balance analysis from our previous study.[11,41,55] By comparison, the BP-1 sample produced a bioethanol yield of 31.01 g, while the bioethanol yield of the BP-2 sample was 23.84 g, and these values were consistent with the distinct hexose yields obtained for the two banana pseudostem samples.

We also conducted biomass processing of the two banana pseudostem samples under the optimal LHW pretreatments (Fig. 3). Compared to the optimal GL pretreatments, the LHW pretreatments led to less hexose and bioethanol yields in both banana pseudostem samples, indicating that the GL pretreatment should be more effective for enhancing lignocellulose saccharification and bioethanol production in banana

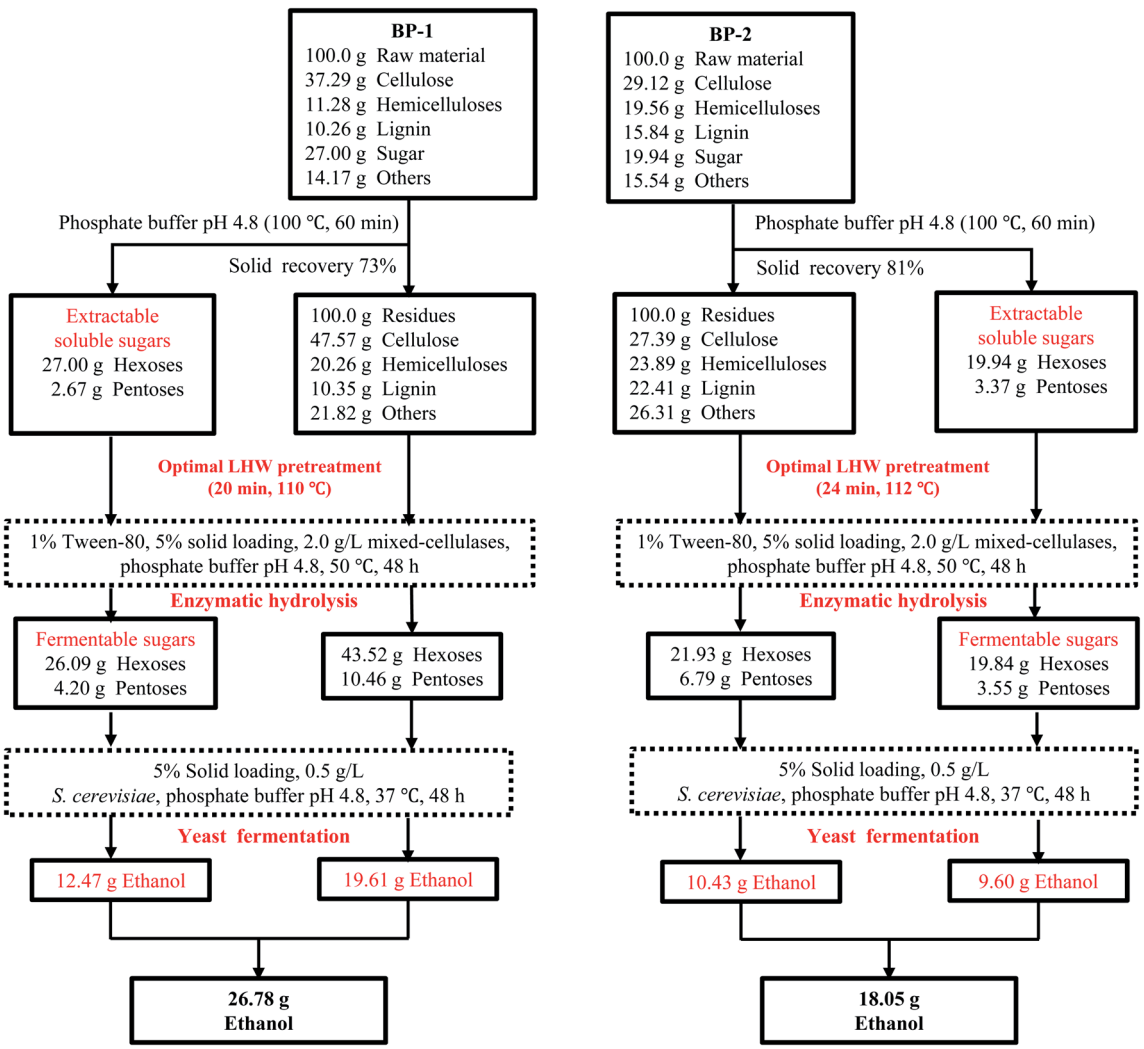

Fig. 3 Mass balance analysis of biomass processing for bioethanol production after performing optimal LHW pretreatments of BP-1 and BP-2 samples.

pseudostems and other crop straws, as previously reported.[41,52] Furthermore, there were higher hexose and bioethanol yields from the BP-1 sample than those from the BP-2 sample under the LHW pretreatments, suggesting that the lignocellulose from the BP-1 sample was less recalcitrant to digestion than that of the BP-2 sample.

In addition, we performed a time course of yeast fermentation using hexoses as a carbon source released from the optimal GL pretreatment with the more optimal banana pseudostem (BP-1) sample (Fig. S1†). We observed that the 48 h yeast fermentation led to the highest bioethanol yield and sugar–ethanol conversion rate achieved in this study, but a longer fermentation of 60 h did not increase either the bioethanol yield or the conversion rate to a significant level ($p < 0.05$). Hence, the yeast fermentation performed in this study was consistent with our previous fermentations.[10–12]

3.3. Comparison of bioethanol production among major bioenergy crops

Although various physical and chemical pretreatments have been implemented in all major bioenergy crops over the past years, their distinct biomass saccharification and bioethanol productivity have not yet been determined. In this study, we thus compared the more optimal banana pseudostem sample (BP-1) with other lignocellulose samples, consisting of a total 12 distinct grassy and woody crops (Table 2). In terms of the biomass enzymatic saccharification, we present the hexose yields against dry matter (% DM) and cellulose (% cellulose). Except for rapeseed stalk and sugarcane bagasse that underwent complete cellulose digestion with hexose yields of 100% (% cellulose), we obtained a hexose yield of 99% for the BP-1 sample under the optimal GL pretreatment, which was a much higher yield than those of other crop residues. Notably, because the BP-1 pseudostem contained much more extractable soluble sugars than those of other lignocellulose residues, the highest bioethanol yield at 31% (% DM) was achieved with the BP-1 sample among all the lignocellulose samples presented. However, the hexose–ethanol conversion rate of the BP-1 sample was relatively lower than those of the other five samples, which may be mainly due to more toxic compounds released *via* yeast fermentation in the biomass processing of the BP-1 sample.[53]

In this study, we only applied 5% solid loading for lignocellulose enzymatic hydrolysis and bioethanol fermentation, which produced bioethanol at relatively low concentrations (g L^{-1}). Thus, an interesting experiment would be to test the

Table 2 Comparison of bioethanol yields achieved in this study and previous studies[e]

		Hexoses								
		Soluble sugars	Enzymatic hydrolysis							
Material	Pretreatment	(% DM[c])	(% DM)	(% cellulose)	Ethanol yield (% DM)	Sugar–ethanol conversion rate (%)	Pentoses (% DM)	Ethanol yield[d] (% DM)	Total ethanol (% DM)	Ref.
Banana pseudostem	**GL[a], 26.7 (%, w/w), 105 °C, 26 min**	**26**	**42**	**99**	**31**	**90**	**16**	**6**	**37**	**This study**
	LHW[b], 110 °C, 20 min	**26**	**32**	**82**	**27**	**91**	**12**	**4**	**31**	
	3% NaOH	ND	40	79	16	80	ND	ND	16	42
	25% NaOH	ND	65	85	ND	ND	5	ND	ND	26
	210 °C, 40 min	ND	35	91	17	95	13	ND	17	29
Rice straw	1 M NaOH, 121 °C, 1 h	ND	26	80	12	91	ND	ND	12	43
Wheat straw	Microwave 300 W, 15 min, 0.2 M H_2SO_4	ND	25	75	11	85	ND	ND	11	44
Cotton stalk	3% NaOH, 121 °C, 130 kPa, 40 min	ND	27	64	6	46	ND	ND	6	45
Rapeseed stalk	Steam explosion, 5% CaO	ND	43	100	21	93	18	6	27	11
Corn straw	LHW, 200 °C, 20 min	24	17	96	19	95	14	5	24	10
Sweet sorghum stalk	12.5% CaO	15	39	90	24	68	8	ND	24	46
Sugarcane bagasse	10% CaO	ND	38	100	19	100	32	ND	19	19
Switchgrass stalk	1% H_3PO_4, 190 °C, 7.5 min	ND	39	42	19	59	16	ND	19	47
Miscanthus straw	0.6 M NaOH	ND	31	78	ND	ND	9	ND	ND	48
Reed straw	LHW, 170 °C, 60 min, Na_2CO_3	ND	36	66	13	65	7	ND	13	49
Poplar stem	150 °C, 45 min, 0.15 M oxalic acid	ND	22	65	8	73	ND	ND	8	50

[a] Green liquor. [b] Liquid hot water. [c] Dry matter. [d] Based on the average xylose–ethanol conversation rate of 35% as previously reported by Rodrussamee *et al.* (2018) and Valinhas *et al.* (2018). [e] ND: not detected.

optimal GL and LHW pretreatments and determine if high concentrations of bioethanol can be produced using the more optimal banana pseudostem sample. In addition, we also estimated the bioethanol yields from xylose co-fermentation with the engineered yeast, based on the average xylose–ethanol conversion rate in theory (Table 2). Because the BP-1 sample also released a high yield of pentoses at 16% (% DM) as a result of enzymatic hydrolysis under the optimal pretreatment, it produced a much higher yield of total bioethanol at 37% (% DM) from both hexose and pentose co-fermentation by the yeast strain. Even though it is difficult to determine a standard for bioethanol yield comparison among different types of biomass residues under various technologies, valuable information would be obtained by investigating how the bioethanol yield would be further increased if advanced process technology was integrated with pretreated lignocellulose substrates.

3.4. Effective cell wall polymer extraction and modification after optimal green-like pretreatments

To understand the distinct enhancements of biomass enzymatic saccharification and bioethanol production as a result of the optimal green-like pretreatments that were performed, we examined the cell wall polymer compositions of the two banana pseudostem samples (Table 3). After the optimal GL pretreatment, the BP-1 sample showed remarkable decreases in lignin and pectin by 40% and 75%, which should lead to relatively increased cellulose and hemicellulose levels by 18% and 17%, respectively, at the $p < 0.01$ level ($n = 3$). The optimal LHW pretreatment reduced the lignin and pectin levels by 25% and 72%, indicating that less lignin was extracted as compared to the optimal GL pretreatment of the BP-1 sample. By comparison, there was relatively less pectin extracted from the BP-2 pseudostem sample after the two green-like pretreatments performed in this study. Nonetheless, only optimal GL pretreatment rather than optimal LHW pretreatment significantly reduced lignin levels by 5% in the BP-2 sample (Table 3). Because lignin deposition has been well characterized as a barrier against enzymatic hydrolysis of cellulose,[15,54] effective lignin extraction by the optimal GL pretreatment would confirm that greatly enhanced enzymatic saccharification of biomass could be accomplished, in particular for the BP-1 pseudostem sample.

Furthermore, we performed attenuated total reflectance-Fourier transform infrared (ATR-FTIR) spectroscopic profiling of the raw material and pretreated biomass residues from the two banana pseudostem samples (Fig. S2†). In the optimal pretreated residues of the two banana pseudostem samples, four characteristic peaks were shifted that correspond to the C–H, C–O–C, C=C, and C=C bonds involved in the lignin interlinkages of the cell wall networks (Table S3†).[33,55–62] One shifted peak was observed that corresponded to interlinkages of hemicellulose with other cell wall polymers. Hence, the data indicated that effective lignin extractions can be achieved by optimal GL and LHW pretreatments in both banana samples. In addition, due to the small amounts of pectin in the banana samples, its corresponding bonds were not detected in this study.

It has been previously shown that cell wall polymer extraction *via* physical and chemical pretreatments increases the cellulose accessibility, resulting in more efficient enzymatic saccharification.[63] Using our recently established approach,[38] Congo red staining indicated that cellulose was accessible in the two banana samples. Upon the two optimal green-like pretreatments, the cellulose accessibility of the pretreated banana samples was greatly increased up to 2-fold as compared to that of their materials at $p < 0.01$ levels (Fig. 4A), which was mainly due to the effective lignin and pectin extractions and altered cell wall polymer interlinkages from the optimal pretreatments described above. Furthermore, the GL pretreatment increased cellulose accessibility to a greater degree than the LHW pretreatment of the two banana samples, which was consistent with their distinct enhancements upon enzymatic saccharification of the banana pseudostem samples (Fig. 2 and 3). Provided that pretreatments can distinctively alter lignocellulose features for subsequent enhancement of biomass enzymatic saccharification,[63,64] we also examined the degree of polymerization (DP) and crystalline index (CrI) of cellulose, which are two major cellulose features that negatively account for lignocellulose recalcitrance.[65,66] Compared to the raw materials, the lignocellulose residues obtained from two optimal green-like pretreatments exhibited cellulose DP values decreased by 19–36% in the BP-1 and BP-2 samples at $p < 0.01$ levels (Fig. 4B). Because cellulose DP is accountable for the amounts of reducing-ends of β-1,4-glucans,[67] the decreased

Table 3 Wall polymer composition (% total) of raw materials and lignocellulose residues obtained from the optimal GL and LHW pretreatments in two banana pseudostem samples[a]

Sample	Pretreatment	Cellulose		Hemicellulose		Lignin		Pectin	
BP-1	Raw material	57.76 ± 0.15		17.47 ± 0.21		15.89 ± 0.16		8.87 ± 0.37	
	GL	67.91 ± 0.42**	17.57%[#]	20.39 ± 0.18**	16.70%	9.48 ± 0.59**	−40.32%	2.22 ± 0.08**	−75.02%
	LHW	61.59 ± 0.64**	6.63%	23.94 ± 0.34**	37.05%	11.95 ± 0.16**	−24.83%	2.52 ± 0.14**	−71.60%
BP-2	Raw material	42.26 ± 0.22		28.39 ± 0.16		22.99 ± 0.17		6.35 ± 0.05	
	GL	47.30 ± 0.61*	11.92%	28.74 ± 0.59		21.83 ± 0.22**	−5.06%	2.13 ± 0.06**	−66.52%
	LHW	43.20 ± 0.51		30.75 ± 0.25**	8.31%	23.74 ± 0.25*		2.31 ± 0.04**	−63.64%

[a] * and ** indicate significant differences between raw materials and pretreated residues by *t*-test at $p < 0.05$ and $p < 0.01$ ($n = 3$). [#] Percentage was calculated by subtraction between raw material and pretreated residue values divided by raw material. Data as mean ± SD ($n = 3$). GL as green liquid; LHW as liquid hot water.

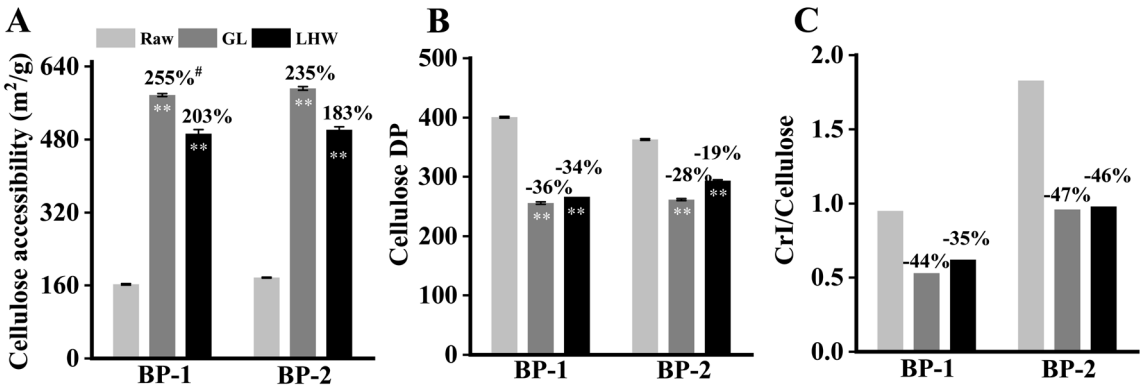

Fig. 4 Characterization of cellulose features (DP, CrI) and accessibility for the BP-1 and BP-2 banana samples after optimal GL and LHW pretreatments. (A) Cellulose accessibility (m^2 g^{-1}) by Congo red staining; (B) cellulose DP; (C) cellulose CrI. # Indicates the percentage of increased/decreased rate between the raw material and pretreated residue by subtraction of two values divided by the raw material. The data are presented as the mean ± SD ($n = 3$). **Indicates the significant difference between the raw material and pretreated residue at the $p < 0.01$ level.

cellulose DP values indicate the de-polymerization degree of cellulose, which should be an important factor for the enzymatic saccharification of the two banana samples that underwent the optimal green-like pretreatments conducted in this work. Our measurements also showed that the cellulose CrI values were decreased by 35–47% in the pretreated lignocellulose residues of the two banana samples, compared with their raw materials (Fig. 4C). Notably, there were consistently lower CrI values for the BP-1 sample as compared to those of the BP-2 sample for the raw materials and their pretreated lignocellulose residues. Because cellulose crystallinity is an integrated factor natively affecting biomass enzymatic saccharification,[68] the results demonstrated that there should be less lignocellulose recalcitrance with the BP-1 sample for the much enhanced biomass enzymatic saccharification and bioethanol production described above.

With respect to the effective lignin extracted from the optimal pretreatments performed in this study, we examined three major lignin monomer proportions in the two banana samples (Fig. S3†). The BP-1 and BP-2 samples exhibited a variation of three monomer ratios (H/G, S/G, S/H) among the raw materials and pretreated lignocellulose residues, which should be mainly due to the distinct lignin extraction under the two optimal green-like pretreatments performed (Table 3). As correlation analysis has been well applied to account for lignin feature impacts on biomass enzymatic digestion under various chemical pretreatments (our study and other references), we were able to determine that the S/H ratio, rather than the S/G and H/G ratios, was significantly correlated with the hexose yields released from enzymatic hydrolyses at the $p < 0.01$ level, which may be influenced by much higher H-monomer levels occurring in the banana lignocellulose residues compared to other major bioenergy crop straws.[69,70] Nevertheless, the S/H ratio could be applied as the unique parameter accountable for banana biomass enzymatic hydrolysis and bioethanol production.

We determined the monosaccharide composition of hemicelluloses in the raw materials and pretreated lignocellulose residues of the two banana samples (Fig. S4†). The banana samples exhibited a high abundance of glucose and arabinose, indicating that the banana pseudostems were rich in xyloglucans, a typical hemicellulose of primary cell walls as previously characterized in banana and other grassy plants.[30,71] In particular, the BP-1 sample contained much more glucose than that of the BP-2 sample in both raw materials and pretreated lignocellulose residues, which should be another factor accounting for their distinct hexose yields released upon enzymatic hydrolyses after two optimal green-like pretreatments were performed. In addition, we noted that the BP-2 samples contained remarkably more xylose than that of the BP-1 in both raw materials and pretreated lignocellulose residues. Xylose is the major monosaccharide of xylan, a typical hemicellulose of secondary cell walls in plants,[72] and the data suggested that the BP-1 and BP-2 pseudostems should contain different proportions of primary and secondary cell walls, which could be attributed to their distinct lignocellulose recalcitrant properties that we observed.

3.5. Mechanism of enhanced bioethanol production in banana pseudostems that underwent optimal green-like pretreatments

To determine why the maximum bioethanol production was achieved in the most optimal banana pseudostem material, we propose a mechanism model that links all the major findings obtained in this study (Fig. 5). First, the model stresses the most optimal banana pseudostem (BP-1) sample rich in directly fermentable soluble sugars and easily digestible xyloglucans. It then demonstrates that the optimal green-like (GL, LHW) pretreatments enabled effective extraction of most pectin and partial lignin for remarkably increased cellulose accessibility in the most optimal pseudostems. Furthermore, the optimal GL pretreatment significantly decreased lignocellulose recalcitrance, and almost complete biomass enzymatic saccharification resulted by largely decreasing cellulose DP and CrI and distinctively altering the hemicellulose and lignin features in the most optimal pseudostem sample.

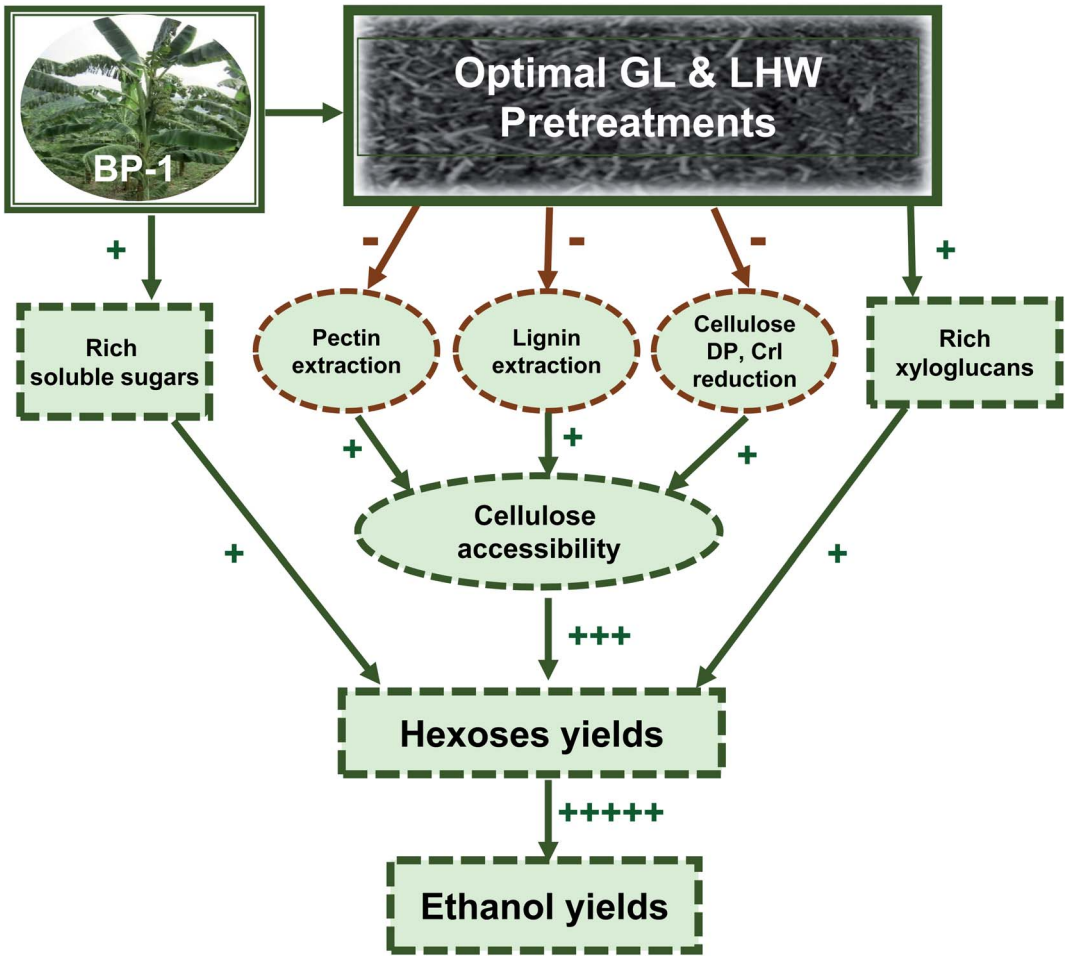

Fig. 5 A hypothetical model that highlights a green-like strategy for the bioethanol industry by integrating engineered bioenergy crops and green-like biomass pretreatments. The engineered bioenergy crop should possess significantly improved cellulose accessibility for efficient enzymatic saccharification with very high soluble sugar accumulation for direct ethanol fermentation. (–) and (+) denote reducing and enhancing strategies, respectively, for biomass processing and bioethanol production in the model.

Finally, we concluded that integration of all hexoses from soluble sugars, xyloglucan, and cellulose should be sufficient to maximize bioethanol yields. Therefore, our model has not only interpreted the major lignocellulose recalcitrant factors that distinctively affect biomass pretreatment and enzymatic saccharification, but we also provide a green-like biomass processing strategy for high bioethanol production using banana pseudostem residues and other bioenergy crop straws.

4. Conclusions

By performing RSM modeling in this study, we established two optimal green-like (GL, LHW) pretreatments for remarkably enhanced enzymatic saccharification of the biomass in two representative banana pseudostem samples. Using pseudostem sample BP-1, which was rich in fermentable sugars (58% hexoses and 17% pentoses; % dry matter), the optimal GL pretreatment (26.74% TTA, 105 °C, 26 min) resulted in almost complete biomass enzymatic saccharification with a hexose yield of 99% (% cellulose), which enabled us to achieve the highest total bioethanol yield of 37% (% dry matter), compared with previously reported total bioethanol yields that ranged from 6% to 27% in the major bioenergy crops examined. Furthermore, we were able to interpret why the maximum bioethanol production was achieved from the optimal green-like pretreatments in the most optimal pseudostem sample by proposing a hypothetical model that connects all the major findings regarding increased extractable soluble sugars and digestible xyloglucans and decreased lignocellulose recalcitrance. Hence, this work provides a green-like strategy for optimal biomass processing to attain maximum bioethanol yields from banana pseudostem residues and other bioenergy crop straws.

Author contributions

Fei Liu: investigation, methodology, formal analysis, writing – original draft. Jingyang Li: investigation, methodology. Hua Yu: validation, data curation. Yuqi Li: investigation, formal analysis. Yanting Wang: validation, project administration. Hairong

Gao: software, formal analysis. Hao Peng: software, methodology. Zhen Hu: editing, formal analysis. Hailang Wang: software. Guifen Zhang: investigation. Yuanyuan Tu: project administration, editing. Liangcai Peng: conceptualization, writing – original draft, writing – review & editing, supervision, funding acquisition.

Conflicts of interest

The authors have no conflicts of interest to declare.

Acknowledgements

This work was supported in part by the Project of Huazhong Agricultural University Independent Scientific & Technological Innovation Foundation (2662020ZKPY013; 2662019PY054), the Earmarked Fund for China Agriculture Research System (CARS-31-02), the Project of Hubei University of Arts & Science (XKQ2018006), and the National 111 Project from the Ministry of Education of China (BP0820035).

References

1 N. Sathitsuksanoh, A. George and Y. Zhang, *J. Chem. Technol. Biotechnol.*, 2012, **88**, 169–180.
2 A. Kumar, *Front. Biosci.*, 2018, **10**, 350–371.
3 M. J. Scully, G. A. Norris, T. M. Alarcon Falconi and D. L. MacIntosh, *Environ. Res. Lett.*, 2021, **16**, 043001.
4 R. A. Holland, F. Eigenbrod, A. Muggeridge, G. Brown, D. Clarke and G. Taylor, *Renewable Sustainable Energy Rev.*, 2015, **46**, 30–40.
5 J. R. Bartle and A. Abadi, *Energy Fuels*, 2010, **24**, 2–9.
6 P. M. A. Pawar, M. Derba-Maceluch, S. L. Chong, L. D. Gómez, E. Miedes, A. Banasiak, C. Ratke, C. Gaertner, G. Mouille, S. J. McQueen-Mason, A. Molina, A. Sellstedt, M. Tenkanen and E. J. Mellerowicz, *Plant Biotechnol.*, 2015, **14**, 387–397.
7 W. Dwianto, F. Fitria, I. Wahyuni, D. S. Adi, S. Hartati, R. Kaida and T. Hayashi, *J. Math. Fundam. Sci.*, 2014, **46**, 169–174.
8 S. Y. Leu and J. Y. Zhu, *BioEnergy Res.*, 2012, **6**, 405–415.
9 D. J. Cosgrove, *Nat. Rev. Mol. Cell Biol.*, 2005, **6**, 850–861.
10 W. Jin, L. Chen, M. Hu, D. Sun, A. Li, Y. Li, Z. Hu, S. Zhou, Y. Tu, T. Xia, Y. Wang, G. Xie, Y. Li, B. Bai and L. Peng, *Appl. Energy*, 2016, **175**, 82–90.
11 L. Wu, S. Feng, J. Deng, B. Yu, Y. Wang, B. He, H. Peng, Q. Li, R. Hu and L. Peng, *Green Chem.*, 2019, **21**, 4388–4399.
12 J. Deng, X. Zhu, P. Chen, B. He, S. Tang, W. Zhao, X. Li, R. Zhang, Z. Lv, H. Kang, L. Yu and L. Peng, *Sustainable Energy Fuels*, 2020, **4**, 607–618.
13 S. Cheng, H. Yu, M. Hu, Y. Wu, L. Cheng, Q. Cai, Y. Tu, T. Xia and L. Peng, *Bioresour. Technol.*, 2018, **263**, 67–74.
14 F. Li, G. Xie, J. Huang, R. Zhang, Y. Li, M. Zhang, Y. Wang, A. Li, X. Li, T. Xia, C. Qu, F. Hu, A. J. Ragauskas and L. Peng, *Plant Biotechnol.*, 2017, **15**, 1093–1104.
15 Z. Hu, G. Zhang, A. Muhammad, R. A. Samad, Y. Wang, J. D. Walton, Y. He, L. Peng and L. Wang, *Sci. Rep.*, 2018, **8**, 3636.
16 Zahoor, D. Sun, Y. Li, J. Wang, Y. Tu, Y. Wang, Z. Hu, S. Zhou, L. Wang, G. Xie, J. Huang, A. Alam and L. Peng, *Bioresour. Technol.*, 2017, **243**, 957–965.
17 K. Shimizu, K. Sudo, H. Ono, M. Ishihara, T. Fujii and S. Hishiyama, *Biomass Bioenergy*, 1998, **14**, 195–203.
18 L. Matsakas, C. Nitsos, V. Raghavendran, O. Yakimenko, G. Persson, E. Olsson, U. Rova, L. Olsson and P. Christakopoulos, *Biotechnol. Biofuels*, 2018, **11**, 160.
19 J. S. Kim, Y. Y. Lee and T. H. Kim, *Bioresour. Technol.*, 2016, **199**, 42–48.
20 M. Hu, H. Yu, Y. Li, A. Li, Q. Cai, P. Liu, Y. Tu, Y. Wang, R. Hu, B. Hao, L. Peng and T. Xia, *Carbohydr. Polym.*, 2018, **202**, 434–443.
21 R. Gonzalez, J. Daystar, M. Jett, T. Treasure, H. Jameel, R. Venditti and R. Phillips, *Fuel Process. Technol.*, 2012, **94**, 113–122.
22 Y. Song, R. P. Chandra, X. Zhang, T. Tan and J. N. Saddler, *Sustainable Energy Fuels*, 2019, **3**, 1329–1337.
23 L. Li, L. Huang, R. J. Linhardt, N. Koratkar and T. Simmons, *Sustainable Energy Fuels*, 2018, **2**, 422–429.
24 B. Satari, K. Karimi and R. Kumar, *Sustainable Energy Fuels*, 2019, **3**, 11–62.
25 J. J. Bhaskar, S. Mahadevamma, N. D. Chilkunda and P. V. Salimath, *J. Agric. Food Chem.*, 2012, **60**, 427–432.
26 S. Basak, K. K. Samanta, S. K. Chattopadhyay and R. Narkar, *Cellulose*, 2015, **22**, 2767–2776.
27 F. L. Shimizu, P. Q. Monteiro, P. H. C. Ghiraldi, R. B. Melati, F. C. Pagnocca, W. d. Souza, C. Sant'Anna and M. Brienzo, *Ind. Crops Prod.*, 2018, **115**, 62–68.
28 S. Díaz, Z. Ortega, A. N. Benítez, D. Costa, F. Carvalheiro, M. C. Fernandes and L. C. Duarte, *Waste Manage.*, 2021, **119**, 306–314.
29 M. Z. Islam, M. A. Asad, M. T. Hossain, S. C. Paul and S. M. A. Sujan, *J. Environ. Sci. Technol.*, 2019, **12**, 157–163.
30 I. Ferreira da Silva, L. Reis Fontinelle Souto, S. R. A. Collins, A. Elliston, J. H. de Queiroz and K. W. Waldron, *BioEnergy Res.*, 2020, **13**, 1159–1170.
31 A. Vijin Prabhu, S. Antony Raja, A. Avinash and A. Pugazhendhi, *Fuel*, 2021, **288**, 119574.
32 J. Wu, R. Chandra and J. Saddler, *Sustainable Energy Fuels*, 2019, **3**, 227–236.
33 L. Peng, C. H. Hocart, J. W. Redmond and R. E. Williamson, *Planta*, 2000, **211**, 406–414.
34 C. Fan, S. Feng, J. Huang, Y. Wang, L. Wu, X. Li, L. Wang, Y. Tu, T. Xia, J. Li, X. Cai and L. Peng, *Biotechnol. Biofuels*, 2017, **10**, 221.
35 C. Fan, H. Yu, S. Qin, Y. Li, A. Alam, C. Xu, D. Fan, Q. Zhang, Y. Wang, W. Zhu, L. Peng and K. Luo, *Biotechnol. Biofuels*, 2020, **13**, 9.
36 Z. Lv, F. Liu, Y. Zhang, Y. Tu, P. Chen and L. Peng, *GCB Bioenergy*, 2020, **13**, 348–360.
37 N. Xu, W. Zhang, S. Ren, F. Liu, C. Zhao, H. Liao, Z. Xu, J. Huang, Q. Li, Y. Tu, B. Yu, Y. Wang, J. Jiang, J. Qin and L. Peng, *Biotechnol. Biofuels*, 2012, **5**, 58.

38 A. Alam, R. Zhang, P. Liu, J. Huang, Y. Wang, Z. Hu, M. Madadi, D. Sun, R. Hu, A. J. Ragauskas, Y. Tu and L. Peng, *Biotechnol. Biofuels*, 2019, **12**, 99.

39 M. Wiman, D. Dienes, M. A. T. Hansen, T. van der Meulen, G. Zacchi and G. Lidén, *Bioresour. Technol.*, 2012, **126**, 208–215.

40 M. Li, S. Feng, L. Wu, Y. Li, C. Fan, R. Zhang, W. Zou, Y. Tu, H. Jing, S. Li and L. Peng, *Bioresour. Technol.*, 2014, **167**, 14–23.

41 A. Alam, Y. Wang, F. Liu, H. Kang, S. Tang, Y. Wang, Q. Cai, H. Wang, H. Peng, Q. Li, Y. Zeng, Y. Tu, T. Xia and L. Peng, *Renewable Energy*, 2020, **159**, 1128–1138.

42 Y. Li, P. Liu, J. Huang, R. Zhang, Z. Hu, S. Feng, Y. Wang, L. Wang, T. Xia and L. Peng, *Green Chem.*, 2018, **20**, 2047–2056.

43 E. L. Souza, G. F. Liebl, C. Marangoni, N. Sellin, M. S. Montagnoli and O. Souza, *Chem. Eng. Trans.*, 2014, **38**, 271–276.

44 M. Takano and K. Hoshino, *Bioresour. Bioprocess.*, 2018, **5**, 16.

45 D. Mikulski and G. Kłosowski, *Biomass Bioenergy*, 2020, **136**, 105528.

46 M. Wang, D. Zhou, Y. Wang, S. Wei, W. Yang, M. Kuang, L. Ma, D. Fang, S. Xu and S. Du, *Fuel*, 2016, **184**, 527–532.

47 M. Kim, K. Han, Y. Jeong and D. F. Day, *Food Sci. Biotechnol.*, 2012, **21**, 1075–1080.

48 W. Wu, V. Rondon, K. Weeks, P. Pullammanappallil, L. O. Ingram and K. T. Shanmugam, *Bioresour. Technol.*, 2018, **251**, 171–180.

49 Y. L. Cha, J. Yang, S. I. Seo, G. H. An, Y. H. Moon, G. D. You, J. E. Lee, J. W. Ahn and K. B. Lee, *Fuel*, 2016, **164**, 322–328.

50 J. Lu, F. Song, H. Liu, C. Chang, Y. Cheng and H. Wang, *Energy*, 2021, **217**, 119332.

51 C. Kundu and J. W. Lee, *J. Ind. Eng. Chem.*, 2015, **32**, 298–304.

52 F. Gu, L. Yang, Y. Jin, Q. Han, H. Chang, H. Jameel and R. Phillips, *Bioresour. Technol.*, 2012, **124**, 299–305.

53 H. Huang, X. Guo, D. Li, M. Liu, J. Wu and H. Ren, *Bioresour. Technol.*, 2011, **102**, 7486–7493.

54 H. Li, Y. Pu, R. Kumar, A. J. Ragauskas and C. E. Wyman, *Biotechnol. Bioeng.*, 2013, **111**, 485–492.

55 D. Jiang, D. Zhuang, J. Fu, Y. Huang and K. Wen, *Renewable Sustainable Energy Rev.*, 2012, **16**, 1377–1382.

56 M. E. Himmel, S. Y. Ding, D. K. Johnson, W. S. Adney, M. R. Nimlos, J. W. Brady and T. D. Foust, *Science*, 2007, **315**, 804–807.

57 R. Kumar, S. Bhagia, M. D. Smith, L. Petridis, R. G. Ong, C. M. Cai, A. Mittal, M. H. Himmel, V. Balan, B. E. Dale, A. J. Ragauskas, J. C. Smith and C. E. Wyman, *Green Chem.*, 2018, **20**, 921–934.

58 H. Guo, C. Hong, X. Chen, Y. Xu, Y. Liu, D. Jiang and B. Zheng, *PLoS One*, 2016, **11**, e0153475.

59 Y. Wang, C. Fan, H. Hu, Y. Li, D. Sun, Y. Wang and L. Peng, *Biotechnol. Adv.*, 2016, **34**, 997–1017.

60 M. Balat, *Energy Convers. Manage.*, 2011, **52**, 858–875.

61 L. Chen, L. Xing and L. Han, *Renewable Sustainable Energy Rev.*, 2009, **13**, 2689–2695.

62 Z. Shi, G. Xu, J. Deng, M. Dong, V. Murugadoss, C. Liu, Q. Shao, S. Wu and Z. Guo, *Green Chem. Lett. Rev.*, 2019, **12**, 235–243.

63 Y. Wang, P. Liu, G. Zhang, Q. Yang, J. Lu, T. Xia, L. Peng and Y. Wang, *Renewable Sustainable Energy Rev.*, 2021, **137**, 110586.

64 R. Roy, M. S. Rahman and D. E. Raynie, *Curr. Res. Green Sustainable Chem.*, 2020, **3**, 100035.

65 W. Jiang, G. Han, C. Zhou, S. Gao, Y. Zhang, M. Li, Y. Gong and B. Via, *J. Wood Chem. Technol.*, 2017, **37**, 359–368.

66 A. F. Tarchoun, D. Trache, T. M. Klapötke and B. Krumm, *Fuel*, 2020, **277**, 118258.

67 D. P. Delmer, M. Thelen and M. P. F. Marsden, *J. Mol. Biol.*, 1984, **3**, 318–356.

68 J. Jia, B. Yu, L. Wu, H. Wang, Z. Wu, M. Li, P. Huang, S. Feng, P. Chen, Y. Zheng and L. Peng, *PLoS One*, 2014, **9**, e108449.

69 L. Oliveira, D. V. Evtuguin, N. Cordeiro, A. J. D. Silvestre, A. M. S. Silva and I. C. Torres, *J. Agric. Food Chem.*, 2006, **54**, 2598–2605.

70 G. Zhang, L. Wang, X. Li, S. Bai, Y. Xue, Z. Li, S. w. Tang, Y. Wang, Y. Wang, Z. Hu, P. Li and L. Peng, *GCB Bioenergy*, 2020, **13**, 305–319.

71 N. Cordeiro, M. N. Belgacem, I. C. Torres and J. C. V. P. Moura, *Ind. Crops Prod.*, 2004, **19**, 147–154.

72 B. P. Lavarack, G. J. Griffin and D. Rodman, *Biomass Bioenergy*, 2002, **23**, 367–380.

